



## Removal of chromium(VI) from aqueous solutions using rubber leaf powder: batch and column studies

Soma Nag<sup>a</sup>, Abhijit Mondal<sup>a</sup>, Umesh Mishra<sup>a</sup>, Nirjhar Bar<sup>b</sup>, Sudip Kumar Das<sup>b,\*</sup>

<sup>a</sup>Department of Chemical Engineering, National Institute of Technology, Agartala, India, emails: [soma.chemical@nita.ac.in](mailto:soma.chemical@nita.ac.in) (S. Nag), [abhijitju17@gmail.com](mailto:abhijitju17@gmail.com) (A. Mondal), [umishra123@rediffmail.com](mailto:umishra123@rediffmail.com) (U. Mishra)

<sup>b</sup>Department of Chemical Engineering, University of Calcutta, Calcutta, India, emails: [nirjhar@hotmail.com](mailto:nirjhar@hotmail.com) (N. Bar), [drsudipkdas@vsnl.net](mailto:drsudipkdas@vsnl.net) (S.K. Das)

Received 28 February 2015; Accepted 12 August 2015

### ABSTRACT

Chromium metal is found in industrial wastewater at a much higher concentration than the prescribed limit set by different regulatory authorities. Since chromium(VI) is very toxic and carcinogenic, it requires removal at source, that is, before its discharge to the water bodies. The present study is carried out for removal of Cr(VI) from aqueous solution by using locally available rubber leaf as a low-cost adsorbent in batch and continuous column mode. The effects of pH, adsorbent dose, contact time, initial metal ion concentration, and temperature on removal of Cr(VI) were studied in batch process. Different kinetic and isotherm models were examined and the model parameters were determined. The column studies were conducted to investigate the effects of flow rate, bed height, and initial metal ion concentration on removal efficiencies. The experimental data reflects reasonably with Thomas and Yoon–Nelson models in continuous mode.

*Keywords:* Rubber leaf; Isotherm; Breakthrough curve; Langmuir model; Freundlich model; Thomas model; Yoon–Nelson model

### 1. Introduction

Water pollution due to the disposal of heavy metals through industrial effluents in the water bodies is a global concern. Heavy metal pollution in water bodies occurs by metal plating, mining operations, battery manufacturing, tannery, ceramic, and glass industries. The wastewater from these industries commonly includes heavy metals like Cd(II), Pb(II), Cu(II), Zn(II), Ni(II), and Cr(VI) etc. The toxic heavy metals are non-biodegradable and when exposed to the

natural eco-system, accumulation of metal ions in human bodies may occur through either direct intake or food chains. Therefore, heavy metals should be prevented from reaching the natural environment and be treated at its source to a safe limit. Chromium is unique among regulated toxic elements in the environment due to its varied toxicity at different oxidation numbers and is treated differently. Chromium exists in +3 and +6 oxidation states, as other oxidation states are not stable in aqueous solution. Chromium(III) is a dietary requirement for a number of organisms. Hexavalent chromium is very toxic to flora and fauna. Health effects related to Cr(VI) exposure include

\*Corresponding author.

diarrhea, stomach and intestinal bleedings, cramps, liver and kidney damage. Hexavalent chromium is mutagenic [1–3].

Chromium and its compounds are discharged in surface water through industries like metallurgical, electroplating, paints and pigments, leather tanning, wood preservation etc. All toxic metal ions are regulated based on their total toxic concentrations, irrespective of their oxidation state. The World Health Organization has established 0.05 mg/l as a maximum allowable concentration of Cr(VI) in drinking water. The concentration of chromium in industrial wastewater varies from 0.5 to 270 mg/l [2] and IS 10500 allows a discharge limit of 2 mg/l in inland surface water [4].

Conventional removal methods have been used are chemical precipitation, coagulation, solvent extraction, filtration, evaporation, ion exchange, membrane separation etc. Due to huge amount of sludge generation, precipitation method creates serious disposal problems [5]. Adsorption of heavy metals on conventional adsorbents, such as activated carbon, has been used widely in many applications as an effective method. However, the high cost of the activation carbon limits its use in wastewater treatment and there is search for low-cost adsorbents. Agricultural waste is one of the rich sources of low-cost adsorbents [6] besides industrial by-products and natural materials. Due to its abundant availability, agricultural wastes, such as peanut husk, rice husk, wheat bran, different kinds of leaves, fruit peels, and seeds are tried by different researchers as low-cost adsorbent for removal of heavy metals from industrial wastewater. Emine et al. [7] studied on pomace—an olive oil industry waste in batch and column studies for removal of Cr(VI) and obtained encouraging results. Bhattacharyya et al. [5] used different industrial waste, activated alumina, neem bark, and saw dust. Singha and Das [8] worked on six different adsorbents of agriculture origin and concluded their usefulness as bio-adsorbents. Excellent adsorption capacity was noticed by Chen et al. [9] for removal of Cr(VI) from aqueous solution in fixed-bed column study using chemically treated corn slack.

A detailed literature survey indicates that rubber leaf powder has most probably not been tried for removal of Cr(VI) so far. Modified Rubber leaf powders were used for removal of Pb(II) and Cu(II) [10,11]. Adsorption capacity of locally available rubber leaf has been explored in this paper for removal of Cr(VI) from aqueous solution in batch and continuous flow packed bed columns.

## 2. Materials and methods

### 2.1. Preparation of adsorbents

Tripura is the second largest natural rubber (*Hevea brasiliensis*) producing state in India. Approximate 1 lakh hectares of land are under rubber production. The plants are fast growing and medium to tall tree (25 m). Leaves are very leathery, smooth and shining, elliptic-oblong, 15–25 cm long. Rubber leaf was collected from a rubber garden near NIT Agartala, Tripura, India and washed thoroughly with double distilled water to remove any dust and mud present. Then it was sun dried for 15 d and grinded in a Philips grinder and dried in an oven at 60°C for 6 h. Finally, it was sieved to obtain desired particle size of –44 +52 mesh (250–350 µm) and kept in desiccators prior to use for adsorption studies.

### 2.2. Preparation of standard Cr(VI) solution

The stock containing 1,000 mg/l of Cr(VI) was prepared by dissolving 2.828 g of A.R grade  $K_2Cr_2O_7$  in 1,000 ml de-ionized water. The stock solution was diluted several times to make the required initial concentrations of Cr(VI) standards and test solutions.

### 2.3. Analysis of chromium(VI) ions

The concentration of chromium(VI) ions in the standard and treated solutions after adsorption was determined by using a UV-Spectrophotometer (Lambda-25 UV-vis, Perkin Elmer, USA) by using 1,5 diphenyl-carbazide as the complexing agent as recommended [12]. The absorbance of the purple-colored solution was read at 540 nm after 10 min. The calibration curve was prepared first with known strengths of dilute Cr(VI) solutions prepared from stock solutions.

### 2.4. Reagents and processes

All the chemicals,  $K_2Cr_2O_7$ ,  $H_2SO_4$ , NaOH, and 1,5 diphenyl-carbazide, were used of analytical grade and obtained from E. Merck India Limited, Mumbai, India. The pH of the solution was measured with a EUTECH make digital microprocessor-based pH meter previously calibrated with standard buffer solutions.

The batch experiments were conducted in 250 ml stoppered Erlenmeyer flask with known strength Cr(VI) solutions. Flask were agitated in an electrically thermostat reciprocating shaker at 120–130 strokes per minute. The test samples were withdrawn at the specific time, filtered, and the filtrate were analyzed for residual Cr(VI) concentration.

The transport of Cr(VI) ion through fixed-bed was explored. The experimental setup comprised of 1.5 cm diameter Perspex column and 50 cm height. Four such columns, in parallel, homogeneously packed with rubber leaf powder, are used simultaneously. The schematic diagram of the experimental setup is shown in Fig. 1. The continuous down flow was maintained by using a multi-channel peristaltic pump; model Master Flex L/S (SN-07528-30) of Cole-Parmer, USA. A constant head was maintained above the bed to avoid channeling of the liquid. The effects of four different flow rates, bed heights, and four different initial metal ion concentrations on breakthrough curves were studied. Samples were collected for analysis from the bottom of the columns initially at 10 min interval for 2 h and thereafter at 30 min interval.

### 3. Results and discussion

#### 3.1. Characterization of the adsorbent

The different physical characteristics of the adsorbents are shown in Table 1. The density was measured by specific gravity bottle and the surface area was measured by BET apparatus, Chemisorb 2720, Micrometrics Instruments Corporation, USA. FTIR analysis was conducted by Nicolet iS10, Thermo Scientific, USA. The point of zero charge of

the adsorbent was determined by solid addition method [13]. Fig. 2(a) and (b) shows the scanning electron micrograph (SEM) (FEI-QUANTA-200, The Netherlands) of the rubber leaf powder before and after adsorption with Cr(VI). The observed image (Fig. 2(a)) shows high roughness and pores on the adsorbent surface. These provide larger effective surface for the easy sorption of Cr(VI) ions. A decrease in the surface roughness is observed in the SEM image of Cr(VI)-loaded rubber leaf and is shown in Fig. 2(b). This shows the adherence of Cr(VI) ions on the adsorbent surface [5,8].

Fig. 3 shows the FTIR plot for fresh and Cr(VI)-loaded rubber leaves and Table 2 represents the shift in the wave number of dominant peak associated with the Cr(VI) loaded in the FTIR plots by comparing between fresh rubber leaves and Cr(VI)-loaded adsorbents. These shift in the wave number indicated that there was metal binding at the surface of the adsorbent [8]. The shift of wave number of  $1,109.35\text{ cm}^{-1}$  (fresh) to  $1,099.71\text{ cm}^{-1}$  (metal loaded) indicated surface  $-\text{OH}$  is one of the functional group responsible for adsorption. Other major functional group responsible for the adsorption are amine ( $1,159.01\text{--}1,167.20\text{ cm}^{-1}$ ), aromatic, acid ( $1,235.18\text{--}1,249.65\text{ cm}^{-1}$ ), carbonyl ( $1,738.99\text{--}1,732.00\text{ cm}^{-1}$ ), and alkene ( $1,642.75\text{--}1,651.73\text{ cm}^{-1}$ ) group present in the adsorbent and some minor shift ester ( $1,020.16\text{--}1,018.23\text{ cm}^{-1}$ ), alkane ( $2,922.59\text{--}2,921.14\text{ cm}^{-1}$  and  $2,848.34\text{--}2,846.49\text{ cm}^{-1}$ ) etc. are also responsible for adsorption.

Crystal radius of Cr(VI) is  $0.52\text{ \AA}$ . It is moderately large ion, fit into the binding site of the natural adsorbents and bind to several group present in the adsorbents simultaneously.

#### 3.2. Batch studies

Batch studies were conducted to investigate the effects of pH, adsorbent dose, contact time, and initial concentration of Cr(VI) ions on metal adsorption. Equilibrium studies were conducted at different Cr(VI) concentrations and at three different temperatures at a constant speed in the electro stated water bath shaker.

##### 3.2.1. Effect of operating parameters

**3.2.1.1. Effect of pH.** The study was conducted taking 100 ml solution in conical flasks, varying pH 1–5 that is below  $p_{\text{pzc}}$  at Cr(VI) concentration of 10 mg/l at  $30^\circ\text{C}$  at a speed of 120–130 strokes per minute. pH of the solution was monitored by adding 0.1 N  $\text{H}_2\text{SO}_4$  or 0.1 N NaOH as per requirement. Fig. 4 shows the effect of pH on removal of Cr(VI). It is noted that

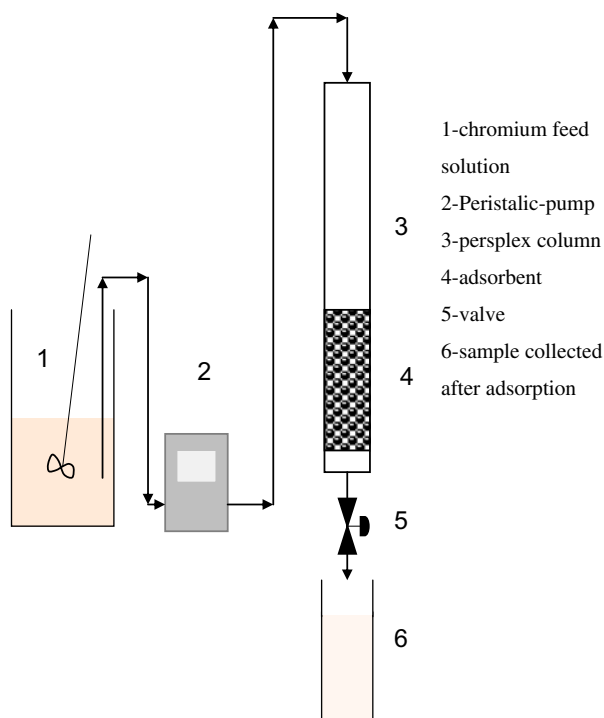


Fig. 1. Experimental setup for column studies.

Table 1  
Characteristic of rubber leaf powder

Particle size mesh	Bulk density (g/cc)	Surface area (unloaded) (m <sup>2</sup> /g)	Surface area (loaded with Cr(VI)) (m <sup>2</sup> /g)	p <sub>zc</sub>	Ash content (dry basis) (%)	Moisture content (dry basis) (%)
–44 +52	0.315	29.17	13.06	7.013	4.50	5.44

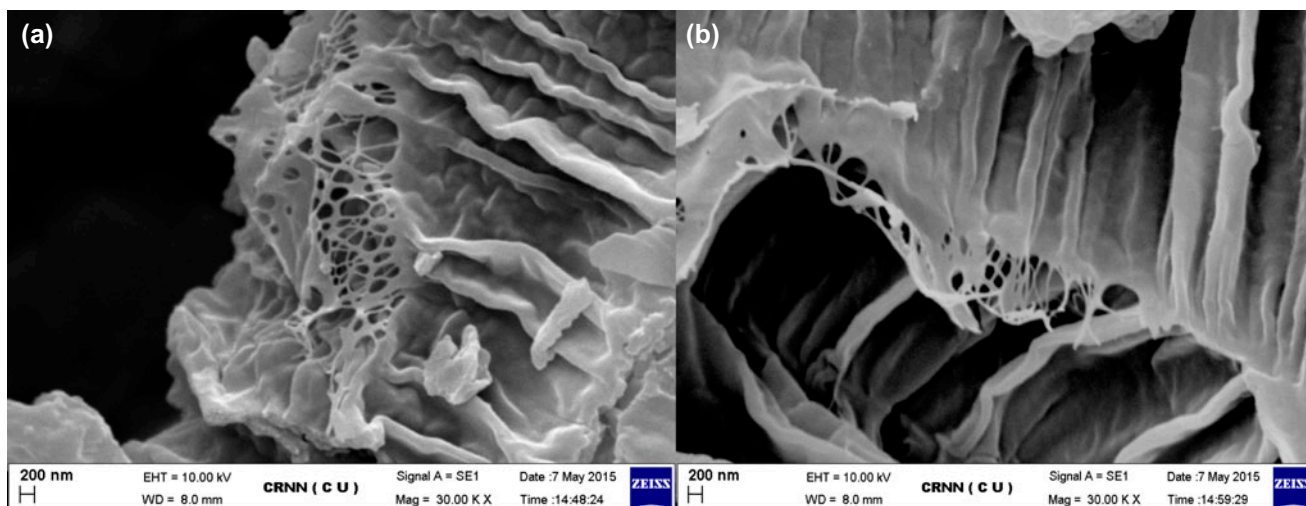


Fig. 2. SEM of the rubber leaf. (a) Raw rubber leaf, and (b) rubber leaf loaded with Cr(VI).

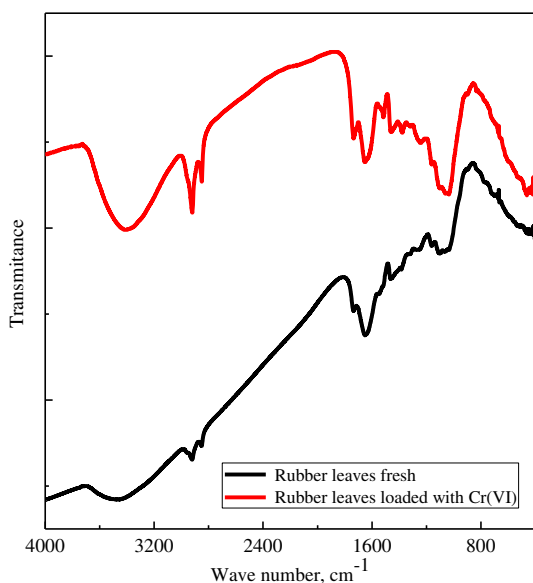


Fig. 3. FTIR analysis for the fresh and Cr(VI)-loaded rubber leaf.

between pH 1–2, removal efficiency is maximum and the highest removal of 98.68% was found at a pH of 1.5. This result is consistent with other researchers

Table 2

Wave number (cm<sup>-1</sup>) for dominant peak from FTIR of adsorption of Cr(VI)

Functional group	Fresh	Cr(VI) loaded
Alcohol O–H stretching	1,109.35	1,099.71
Amine C–N stretching	1,159.01	1,167.20
Aromatic C=C stretching	1,382.23	1,368.25
Acid C–O stretching	1,235.18	1,249.65
Carbonyl C=O stretching	1,738.99	1,732.00
Alkene C=C stretching	1,642.75	1,651.73
Alkane C–H stretching	2,922.59	2,921.14
Alkane C–H stretching	2,848.34	2,846.49
Ester C–O stretching	1,020.16	1,018.23

[14–16]. This may be due to the fact that at pH ≤ 1.0, the dominant form of Cr(VI) is H<sub>2</sub>CrO<sub>4</sub> [17] and increase in pH shifts the concentration of HCrO<sub>4</sub><sup>-</sup> to Cr<sub>2</sub>O<sub>7</sub><sup>2-</sup> and CrO<sub>4</sub><sup>2-</sup>. At low pH, a large number of H<sup>+</sup> ions are present, which neutralizes the OH<sup>-</sup> ions on the adsorbent surface and facilitating diffusion and adsorption of Cr(VI) ions on the adsorbent surface [5]. Above pH 2, the removal percentage falls sharply and reaches to 21.7% at pH 5 due to the overall surface charge on the biosorbents become negative and hence adsorption decreases [18]. The same trend was also

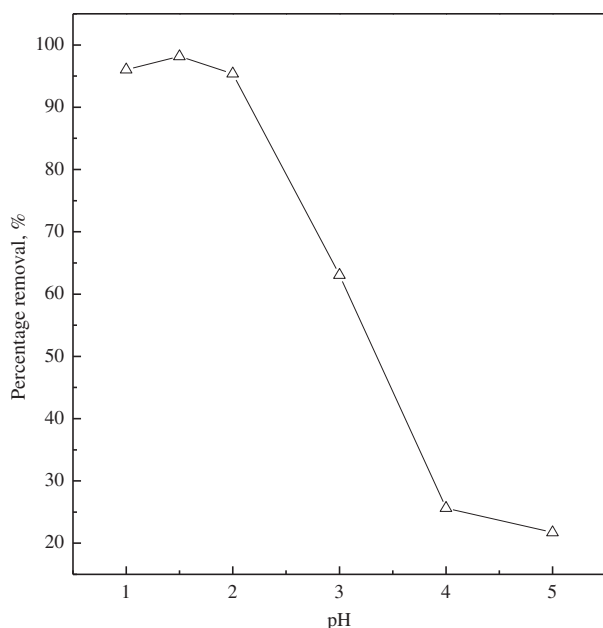


Fig. 4. Effect of pH on removal of Cr(VI): initial Cr(VI) concentration 10 mg/l, adsorbent dose 5 g/l, contact time 4.5 h.

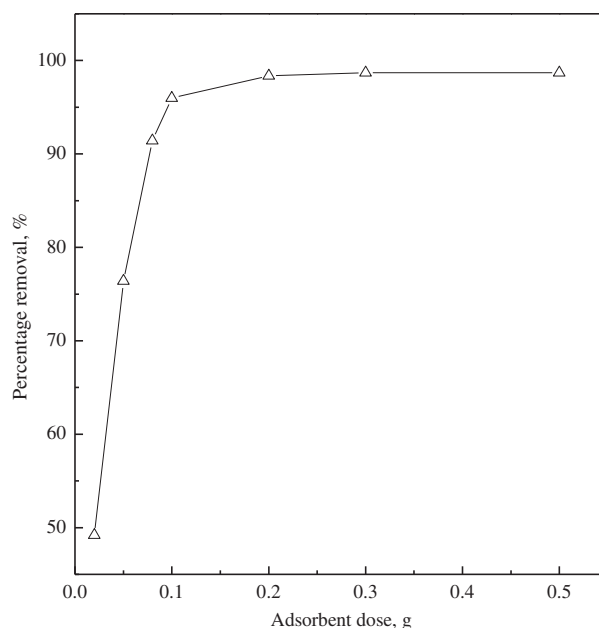
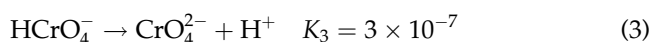


Fig. 5. Effect of adsorbent dose on Cr(VI) removal: initial concentration 10 mg/l, pH 1.5, contact time 4.5 h.

reported by other researchers [5–8]. The following equilibrium exist for Cr(VI) anions in aqueous solutions:



Adsorption of Cr(VI) was not significant at higher pH (pH > 6) due to the formation of complex of anions  $\text{Cr}_2\text{O}_7^{2-}$ ,  $\text{CrO}_4^{2-}$ ,  $\text{OH}^-$  which adsorbed on the adsorption surface [18–20]. This study helped in designing the appropriate pH of the effluent/wastewater to achieve maximum efficiency for removal of Cr(VI) by rubber leaf powder. In future studies, the aqueous solution pH was maintained at 1.5 to get the optimum adsorption.

**3.2.1.2. Effect of adsorbent dose.** Effect of adsorbent dose is shown in Fig. 5 and it showed that, initially, percent removal increased at a very fast rate with the increase in adsorbent concentration and reaches to 98.68% at a concentration of 2 g/l and thereafter it did not increase so significantly. It may be explained that with increase in adsorbent dose, more surface area was

available for adsorption, so the removal efficiency increased. At concentration of adsorbent increased, equilibrium the metal ion adsorption capacity,  $q_e$ , decreased. At 2 g/l, adsorption capacity was 9.6 mg/g and at 5 g/l, it fell down to 1.97 mg/g against 98.68% removal. Since optimum removal efficiency was found at an adsorbent concentration of 2 g/l, it was maintained for rest of the experiments. This reduces the usages of adsorbent quantity and hence is more economical.

**3.2.1.3. Effect of initial metal ion concentration.** Fig. 6 shows that the Cr(VI) removal percentage is decreased with increase in initial metal ion concentration. Removal efficiency gradually falls with increase of Cr(VI) concentration and drops to 85.82% at 50 mg/l concentration level. The possible reason may be that at lower concentration level, adsorption takes place at higher active sites of the adsorbent and as concentration of metal ion increases, adsorption is to take place at lower active sites and thus adsorption decreases [5]. However, equilibrium adsorption capacity,  $q_e$ , increased from 2.49 mg/g at 5 mg/l solution to 21.45 mg/g at a concentration of 50 mg/l as mass transfer increased due to higher concentration level of metal ions. Cr(VI) concentration,  $C_e$ , was measured as 7.47, 3.347, and 0.386 mg/l at 30, 40, and 50°C, respectively, for Cr(VI) initial concentration of 50 mg/l at equilibrium.

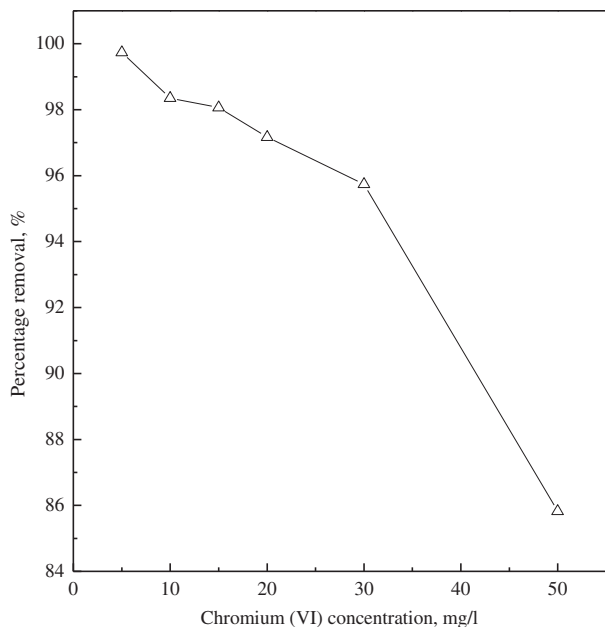


Fig. 6. Effect of initial Cr(VI) concentration on removal: adsorbent dose 2 g/l, pH 1.5, contact time 4.5 h.

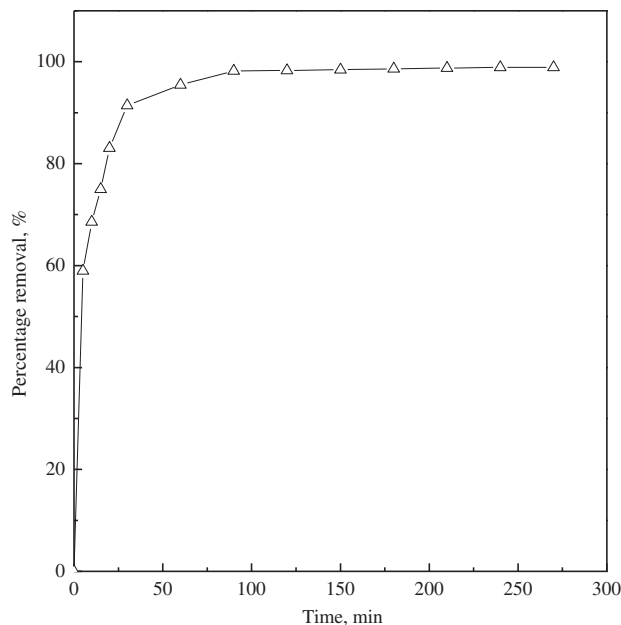


Fig. 7. Effect of contact time on Cr(VI) removal: initial Cr (VI) concentration 10 mg/l, adsorbent dose 2 g/l, pH 1.5.

3.2.1.4. *Effect of contact time.* The effect of contact time on batch adsorption of at 30°C is shown in Fig. 7. It shows that the reaction 90% adsorption was completed within 1 h. Thereafter, the reaction rate became very slow and reaches equilibrium in nearly three hours. However, contact time of 4.5 h was chosen uniformly for all experiments to attain equilibrium.

### 3.2.2. Adsorption kinetic study

Predicting rate of adsorption is the most important factor in adsorption system design.

The kinetic study described the solute uptake rate and evidently this rate controlled the residence time of adsorbate uptake at the solid-solution interface including the diffusion process. This mechanism depends on the physical and chemical characteristics of the adsorbents and also the mass transfer process [8]. Several kinetic models are available to represent the order of the reaction based on solute concentration. The reaction orders may be specified based on different kinetic models. Kinetic models, namely, pseudo-first-order, pseudo-second-order models were tried and rate limiting step was predicted. The reaction kinetics was studied at 30°C with initial metal ion concentration of 10 mg/l and at an adsorbent dose of 2 mg/l with an average shaking speed of 120–130 strokes per minute. The solute uptake was controlled by the metal ion diffusion rate on the adsorbent

surface and the mechanism of adsorption depends upon physical and chemical characteristics of the adsorbents.

The pseudo-first-order model was proposed by Lagergren [21]. The model assumes that the adsorption is diffusion-controlled and the integral form of the model is expressed as:

$$\log(q_e - q) = \log q_e - \frac{K_{ad}t}{2.303} \quad (4)$$

The parameters were obtained from the plot of  $\log(q_e - q)$  vs. time and shown in Fig. 8 and Table 3 shows the parameters with statistical analysis.

The pseudo-second-order model [22] assumes that chemisorption takes place on the adsorbent surface. The linear form of pseudo-second-order equation is expressed by:

$$\frac{t}{q} = \frac{1}{K_2q_e^2} + \frac{t}{q_e} \quad (5)$$

The parameters can be determined from the plot of  $t/q$  vs.  $t$  and shown in Fig. 9 and the values are shown in Table 3. From Table 3, it can be concluded that the pseudo-second-order model fits the experimental data well. This means that the chemical interaction between the adsorbent sites and Cr(VI) ions could be the sole rate-determining step [23].

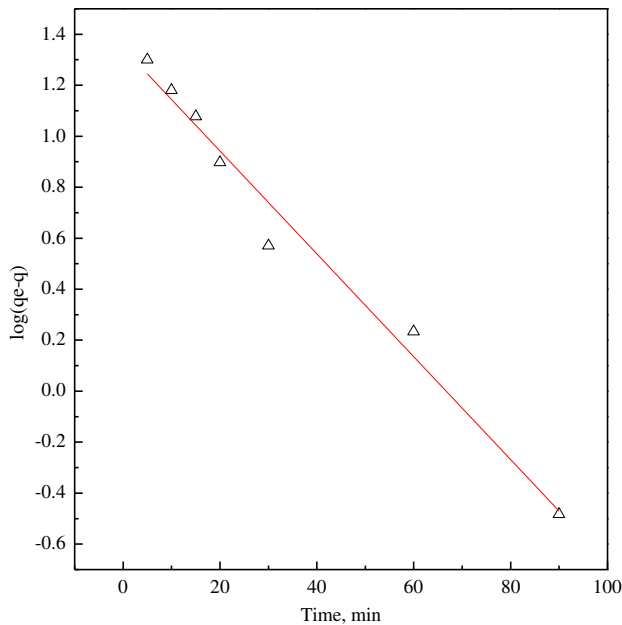


Fig. 8. Lagergren plot for adsorption of Cr(VI): initial Cr (VI) concentration 10 mg/l, adsorbent dose 2 g/l, pH 1.5.

### 3.2.3. Prediction of adsorption rate-limiting step

The adsorbate transport from solution phase to the adsorbent surface takes place in several steps. First, transport to solute from the solution phase to the surface of the adsorbent by mass transfer through the

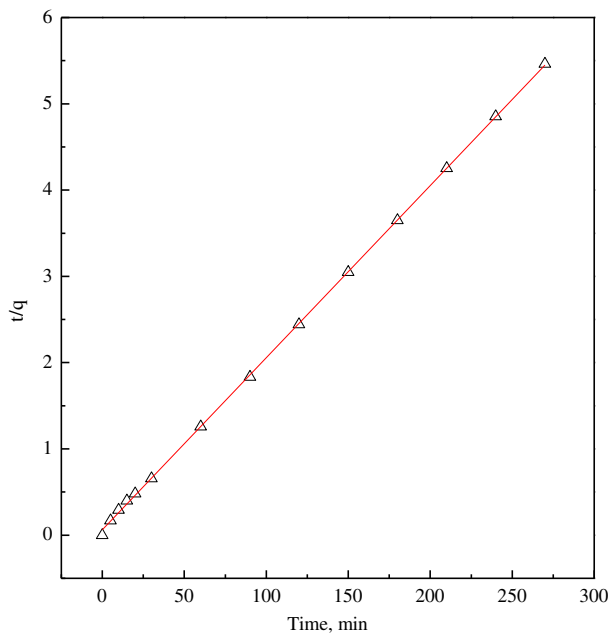


Fig. 9. Pseudo-second-order plot for adsorption of Cr(VI): initial concentration 10 mg/l, adsorbent dose 2 g/l, pH 1.5.

boundary layer which is known as film diffusion. Second step is diffusion of the solute to the surface and pores of the solid. This is called intra-particle diffusion and the last step is adsorption reaction on to the active groups in inner and outer surface of adsorbent. Generally, the inner or outer diffusion controls the adsorption rate. To describe the diffusion process of Cr(VI) ions on the microspheres, Fick's equation is attempted and is given by [8]:

$$\frac{q_t}{q_e} = \frac{6}{R_a} \sqrt{\frac{D_e t}{\pi}} \quad (6)$$

$q_\infty$  is replaced by  $q_e$  and the plot of  $q_t/q_e$  vs.  $t^{0.5}$  of experimental data shows multi-linear segments as depicted in Fig. 10. The first steeper portion represents that the adsorption is diffusion mass transfer controlled and the second linear portion gives an idea of intra-particle diffusion domination in that part [8]. The last linear portion related to adsorption-desorption equilibrium. The first linear portion took 30 min and the second linear portion took 60 min. The ratio of the time taken by film diffusion to intraparticle diffusion is 1:2. So, it can be concluded that intraparticle diffusion is predominant over the film diffusion and intraparticle diffusion is the rate-controlling step.

### 3.2.4. Mass transfer analysis

Mass transfer analysis for removal of Cr(VI) from aqueous solution was carried out using the following equation [24]:

$$\ln\left(\frac{C_t}{C_0} - \frac{1}{1 + MK_{bq}}\right) = \ln\left(\frac{MK_{bq}}{1 + MK_{bq}} - \frac{1 + MK_{bq}}{MK_{bq}}\right) \beta S_s t \quad (7)$$

The plot of  $\ln(C_t/C_0 - 1/1 + MK_{bq})$  vs.  $t$  yields a straight line and from the slope,  $\left(\frac{1 + MK_{bq}}{MK_{bq}}\right) \beta S_s$ , the value of mass transfer co-efficient ( $\beta$ ) was calculated. Value of mass transfer co-efficient was estimated to be  $10.51 \times 10^{-4}$  cm/s with a correlation co-efficient of 0.95 for initial Cr(VI) ion concentration of 10 mg/l. The value of mass transfer co-efficient indicates that the mass transfer rate for the liquid phase to the solid phase was quite fast.

### 3.2.5. Equilibrium studies

The equilibrium studies were conducted varying initial Cr(VI) ion concentration from 5 to 50 mg/l at

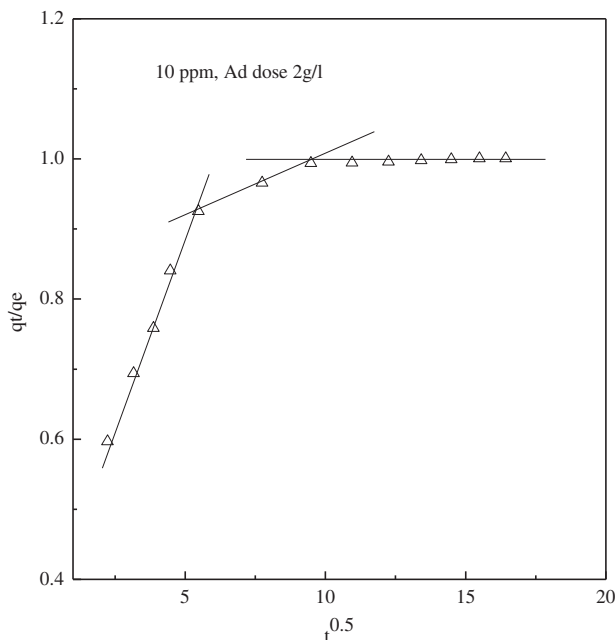


Fig. 10. Plot of  $q_t/q_e$  vs.  $t^{0.5}$  for adsorption of Cr(VI): initial Cr(VI) concentration 10 mg/l, adsorbent dose 2 g/l, pH 1.5.

30–50°C at adsorbent dose level of 2 g/l and the adsorption equilibrium data are represented by Langmuir and Freundlich isotherm models. Adsorption isotherms indicate the qualitative information on the nature of the solute–surface interaction and also relation between the concentration of adsorbate and its degree of accumulation onto adsorbent surface. Adsorption isotherms are used to optimize the use of adsorbents and the analysis of the isotherm data fitting them to different isotherm models is an important step to find the suitable model which can be used for scale-up design [25,26].

**3.2.5.1. Langmuir isotherm model.** Langmuir [27] model assumes monolayer adsorption with a finite number of adsorption sites. Linearity of the plot indicates the application of the isotherm. The equation is commonly written as follows:

$$\frac{C_e}{q_e} = \frac{C_e}{q_{\max}} + \frac{1}{q_{\max}b} \quad (8)$$

The linear plot of  $C_e/q_e$  vs.  $C_e$ , is shown at Fig. 11. From the slope and intercept, the values of  $q_{\max}$  and  $b$  are determined and tabulated at Table 4. The essential characteristics of Langmuir isotherm may be expressed in terms of a dimensionless constant, called separation factor [8],  $R_L$ , which is defined as:

$$R_L = \frac{1}{1 + bC_0} \quad (9)$$

The  $R_L$  value lying between 0 and 1 indicates strong affinity for adsorption. The  $R_L$  value varied from 0.011 to 0.1 for initial concentration 5 to 50 mg/l at 30–50°C. Hence, it indicates favorable adsorption.

**3.2.5.2. Freundlich isotherm model.** It is based on the assumption that adsorbent had a heterogeneous surface composed of different classes of adsorption sites. Freundlich equation is as follows:

$$\log q_e = \log K_f + \frac{1}{n} \log C_e \quad (10)$$

$K_f$ , the Freundlich adsorption capacity and  $n$ , the Freundlich isotherm constant, is an empirical parameter that varies with degree of heterogeneity and its values lie between 1 and 10 for favorable adsorption [7]. The constants were calculated from the Freundlich plot as shown in Fig. 12. The values of the constants are provided in Table 4. The  $n$  values lie between 1 and 10, it indicates favorable adsorption. From Table 3, it is clear that statistical parameter indicated that Langmuir model fitted better than the Freundlich model. This indicates that the adsorption occurs on the homogeneous surface by monolayer adsorption and is described by chemisorption due to formation of

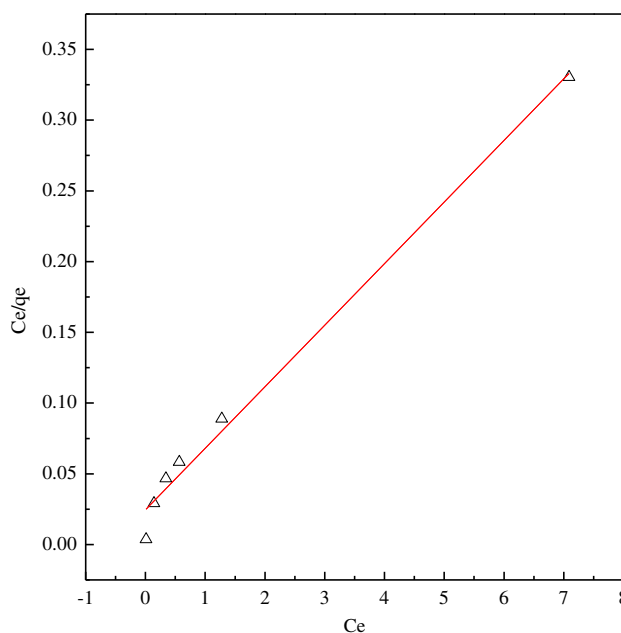


Fig. 11. Langmuir plot for adsorption: initial Cr(VI) concentration 10 mg/l, adsorbent dose 2 g/L, pH 1.5.

Table 3  
Reaction kinetics data

Pseudo-first-order rate constant			Pseudo-second-order rate constant			Mass transfer analysis	
$K_{ad}$ ( $\text{min}^{-1}$ )	$q_e$ ( $\text{mg/g}$ )	Correlation coefficient ( $R^2$ )	$K_2$ ( $\text{mg/g/min}$ )	$q_e$ ( $\text{mg/g}$ )	Correlation coefficient ( $R^2$ )	Mass transfer coefficient $\beta$ ( $\text{m/s}$ )	Correlation coefficient ( $R^2$ )
0.46	32.13	0.9769	$6.46 \times 10^{-3}$	50.12	0.9998	$10.51 \times 10^{-4}$	0.9521

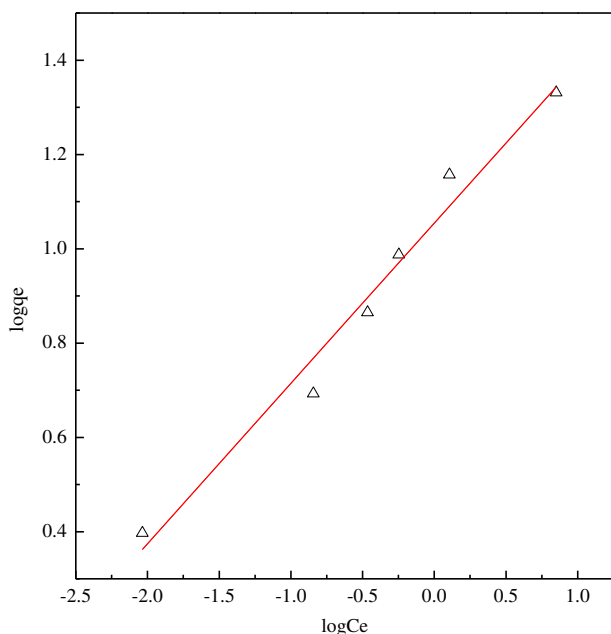


Fig. 12. Freundlich plot for adsorption

ionic or covalent bonds between the adsorbents and adsorbate [14].

3.2.5.3. *Dubinin–Radushkevich isotherm model* [28]. The nature of adsorption process may be predicted by this model. The linear form of model is described by:

$$\ln C_{\text{abs}} = \ln X_m - \lambda \varepsilon^2 \quad (11)$$

where the Polani potential,  $\varepsilon$ , is given by:

$$\varepsilon = RT \ln \left( 1 + \frac{1}{C_e} \right) \quad (12)$$

From the plot of  $\ln C_{\text{abs}}$  vs.  $\varepsilon^2$ , the values of  $\lambda$  and  $X_m$  are calculated from slope and intercept, respectively. The mean sorption energy,  $E$ , was evaluated from:

$$E = \frac{1}{\sqrt{-2\lambda}} \quad (13)$$

The calculated value of the sorption energy,  $E$  (kJ/mol), gives an information about the nature of adsorption process, whether physical or chemical. If the value of  $E$  is less than 8 kJ/mol, the process is physical adsorption and the values between 8 and 16 kJ/mol the process is chemisorption. The estimated value came to 8.45 kJ/mol at 30°C, which indicated the process was chemisorption [8,29].

### 3.2.6. Thermodynamic studies

To see the effects of temperature, adsorption studies were conducted at temperatures 30–50°C, varying initial metal ion concentration from 5 to 50 mg/l at an adsorbent dose level of 2 g/l. The heterogeneous equilibrium was established between the Cr(VI) in the solution and Cr(VI) on the adsorbent. The apparent equilibrium constant,  $K'_c$  was calculated by Eq. (11) at different initial concentrations and then extrapolating to zero to get  $K_c^0$ . The thermodynamic parameters, such as Gibbs free energy ( $\Delta G^\circ$ ), enthalpy ( $\Delta H^\circ$ ), and entropy ( $\Delta S^\circ$ ) (J/mol) on adsorption of Cr(VI) on rubber leaf powder were determined by using the following equations:

$$K'_c = \frac{C_{\text{ad,eq}}}{C_{\text{eq}}} \quad (14)$$

$$\Delta G^\circ = -RT \ln K_c^0 \quad (15)$$

The Gibbs free energy ( $\Delta G^\circ$ ) is calculated from Eq. (9) and given in Table 5. The negative value of free energy suggests that the adsorption process is spontaneous and its further decrease with temperature increase indicates that the spontaneity increases with increase in temperature. The enthalpy ( $\Delta H^\circ$ ) and entropy were calculated from the slope and the intercept of the plot of  $\ln K_c^0$  vs.  $1/T$  and shown in Fig. 13.

$$\ln K_c^0 = -\frac{\Delta H^\circ}{RT} + \frac{\Delta S^\circ}{R} \quad (16)$$

Table 4  
Isotherm values

Temperature	Langmuir constants			Freundlich constants		
	$q_{\max}$ (mg/g)	$b$	$R^2$	$K_f$ (mg/g)/(mg/l) <sup>1/n</sup>	$n$	$R^2$
30°C	22.97	1.18	0.988	12.88	3.58	0.876

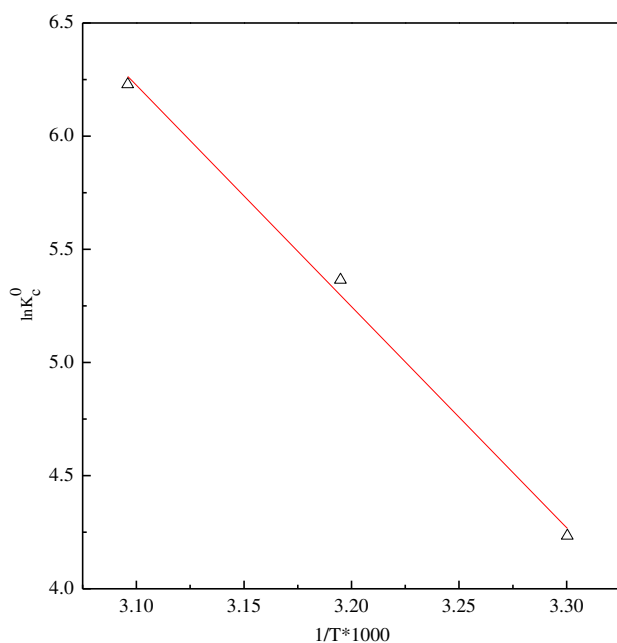


Fig. 13.  $\ln K_c^0$  vs.  $1/T$  plot.

The enthalpy was calculated to be 81.22 kJ/mol and entropy was 303.54 J/mol K. Positive values of enthalpy and entropy change suggest the adsorption process was endothermic and random in nature. Moreover, the value of enthalpy change suggests that the adsorption of Cr(VI) on rubber leaf powder was chemisorption in nature as it lies between 40 and 800 kJ/mol [30].

### 3.2.7. Desorption studies

The weakly bonded Cr(VI) ions with the rubber leaf were removed by using alkaline solution to form soluble chromate [31,32]. After adsorption, the used rubber leaf powder was regenerated by washing it with 0.5 N NaOH solution and then by distilled water and oven dried. The regenerated powder was again used in batch process under same operating conditions and the removal percent of Cr(VI) was obtained 91.57% against 97.0% for the fresh rubber leaf for an initial concentration of 16.5 ppm and adsorbent dose

of 2 g/l at pH 1.5 at 30°C. After second regeneration, the removal percentage further decreased and the overall performance is presented in Table 6.

### 3.2.8. Comparison of adsorbent capacity with different adsorbents reported in literature

The adsorption capacity of Cr(VI) onto different natural adsorbents were compared with other adsorbents reported in literature and is shown in Table 6. The adsorption capacity varies and it depends on the characteristics of the individual adsorbent and initial concentration of the adsorbate. Results of our investigation revealed that rubber leaf has potential to be used for the removal of Cr(VI) ions from aqueous solution (Table 7).

### 3.3. Continuous column adsorption studies

Adsorption in fixed-bed columns are often used in industry due to several advantages like handling of bulk quantities of liquids and efficient use of adsorbents. But the bed does not attain equilibrium while discharging liquid in continuous flow mode. So the batch experimental data cannot be used directly for scale up in columns. The major characteristic of continuous fixed-bed column is the history of the effluent concentration. These concentration-time curves are commonly known as breakthrough curves. The rational design of the fixed-bed column system is based on accurate predictions of the breakthrough curves under specific operating conditions. The fixed-bed analysis in general is very complex. The operation depends on equilibrium (isotherm and capacity), kinetics (diffusion and convective coefficients), and hydraulic (liquid holdup, geometric analysis, and maldistribution) factors [41,42].

The column performance was evaluated by plotting relative concentration of Cr(VI) ion, which is defined as the ratio of the concentration of Cr(VI) ion in effluent to the concentration in Cr(VI) ion in influent ( $C_t/C_0$ ) with respect to flow time,  $t$ . The total Cr(VI) ion adsorbed,  $q_t$ , in the fixed-bed column for a given solute concentration and flow rate is calculated from the following equation:

Table 5  
Thermodynamic parameters

Temperature (°C)	$-\Delta G^\circ$ (kJ/mol)	$\Delta H$ (kJ/mol)	$\Delta S$ (J/mol/°C)
30	10.65	81.22	303.54
40	13.96		
50	16.73		

Table 6  
Desorption studies

Adsorbent	% Removal of Cr(VI)
Fresh rubber leaf	97
After 1st regeneration	91.57
After 2nd regeneration	79.4

$$q_t = \frac{v}{1,000} \int_{t=0}^{t=t_s} C_{ad} dt \quad (17)$$

The equilibrium uptake of Cr(VI) ions,  $q_{eq}$ , based on the weight of the biomass can be calculated from the following equation:

$$q_{eq} = \frac{q_t - q_{t0}}{\chi} \quad (18)$$

The percentage of removal ( $R$ ) can be calculated from the following equation:

$$R = \frac{C_0 - C_t}{C_0} \times 100 \quad (19)$$

### 3.3.1. Effect of the operating parameters

**3.3.1.1. Effect of flow rate on breakthrough curves.** The breakthrough curves at various flow rates (5, 10, 15, and 20 ml/min) are shown in Fig. 14 at a bed height of 5 cm, equivalent to 2.5 g of adsorbent. The curves show that earlier breakthrough is reached with increase in flow rate. The equivalent metal uptake capacity is also influenced by the flow rate. The breakthrough curves become steeper with flow rate and the breakthrough time decreases. The removal efficiency of Cr(VI) is reduced. The uptake capacity of 17.5 and 20.18 mg/g was recorded at velocity of 5 and 20 ml/l, respectively, and the percentage removal decreased from 100 to 26.89% at the initial Cr(VI) concentration of 10 mg/l. This shows that at high flow rates, the adsorption capacity was lower due to residence time being low and also the diffusion of the solute into pores of the adsorbent and hence the solution leaves

Table 7  
Langmuir adsorption capacity for various low-cost natural adsorbents

Sl. No.	Adsorbents	Adsorbent capacity for Cr(VI) (mg/g)	Refs.
1	Saw dust	20.7	[5]
2	Neem bark	19.60	[5]
3	Rice straw	12.172	[8]
4	Rice bran	12.341	[8]
5	Rice husk	11.398	[8]
6	Hyacinth root	15.281	[8]
7	Neem leaves	15.954	[8]
8	Coconut shell	18.695	[8]
9	Sugar beat pulp	17.02	[33]
10	Hazelnut shell	17.70	[34]
11	Almond shells	10.616	[35]
12	Cactus leaves	7.082	[36]
13	Coconut tree sawdust	3.6	[37]
14	Wheat bran	0.942	[38]
15	Coconut husk fibers	29	[39]
16	Waste tea	1.55	[40]
17	Pine leaves	0.277	[41]
18	Rubber leaves	22.97	Present study

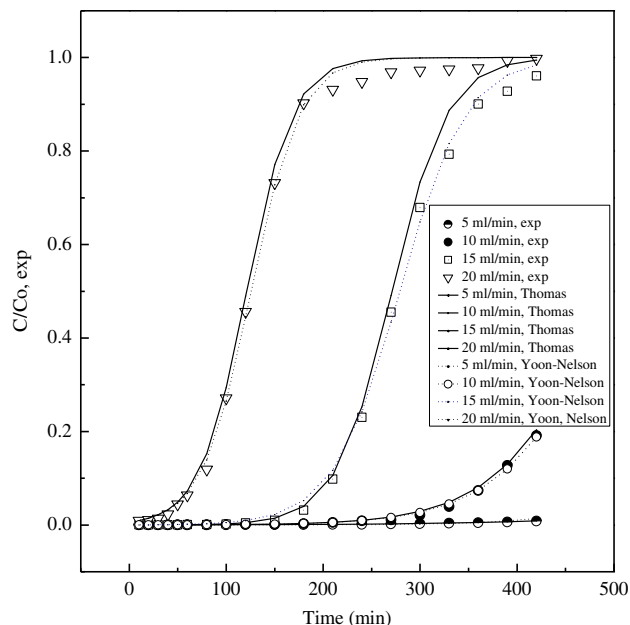


Fig. 14. Effect of flow rate on breakthrough performance and comparison with Thomas model and Yoon–Nelson model: pH 1.5, effluent concentration: 10 mg/l, bed height: 5 cm and flow rate: 15 ml/min.

the column before reaching the equilibrium [41,43]. Hence, lower flow rates are suggested for effective removal of Cr(VI) from wastewater in fixed-column mode.

**3.3.1.2. Effect of bed depth on the breakthrough curve.** The breakthrough curves at different bed heights are shown in Fig. 15. From the figure, it was noted that with the increase in bed height, the Cr(VI) ions get in contact with more adsorbent, hence higher removal efficiency was observed. So at higher bed heights, decrease in concentration of Cr(VI) in the effluent was observed. The slope of the breakthrough curves decreased with increase in bed height as the mass transfer zone increased [30]. Higher metal uptake capacity of 18.89 mg/g was observed at the bed height of 3 cm and the uptake was reduced to 9.42 at 9 cm bed height due to availability of more adsorbents, that is, more surface area [41].

**3.3.1.3. Effect of initial Cr(VI) concentration on the breakthrough curve.** The breakthrough curves at different initial Cr(VI) concentrations are shown in Fig. 16. From the figure, it was noted that with the increase in initial concentration, breakthrough curves become sharper. As more Cr(VI) ions come in contact with adsorbent, lower removal efficiency was observed. Removal percentage decreased from 76.87 to 54.09%

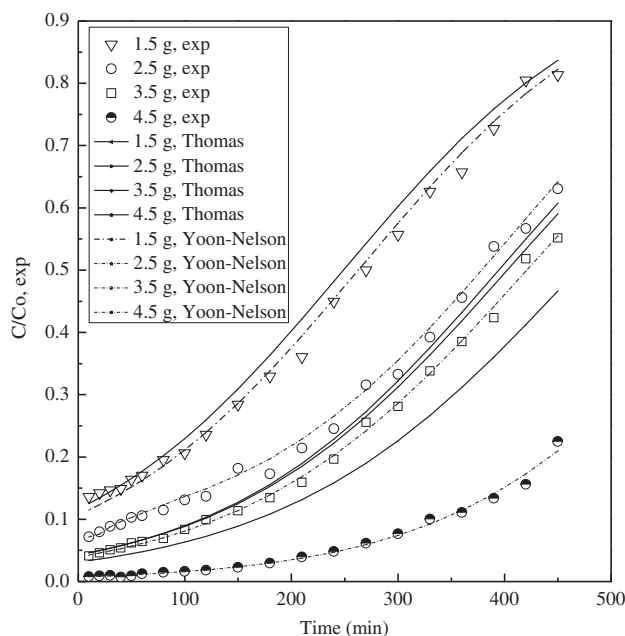


Fig. 15. Effect of bed height on breakthrough performance and comparison with Thomas model and Yoon–Nelson model: flow rate: 15 ml/min, pH 1.5, effluent concentration: 10 mg/l.

with increase in concentration from 5 to 20 mg/l at a flow rate of 15 ml/min and 7 cm bed height. Metal uptake increased from 6.89 to 17.76 mg/g with increase in initial metal ion concentration due to increased mass transfer rate at higher concentration. The similar results were obtained by other researchers [44–48].

### 3.3.2. Modeling of breakthrough curves

The performance of a fixed-bed column may be represented by breakthrough curves. Modeling of adsorption dynamics of the column are based on mass balance across an infinitesimal element in the normal to the direction of flow. The axial and radial dispersion are neglected. Several empirical models, like, Thomas model, Yoon–Nelson model, Bohart–Admas model etc. are available for breakthrough curve prediction. In this paper, first two models are discussed and the model parameters are determined. The experimental breakthrough curves are also compared with the model predicted curves which show reasonable good fittings.

**3.3.2.1. Thomas model [48].** Thomas model is one of the most widely used models. The Thomas model,

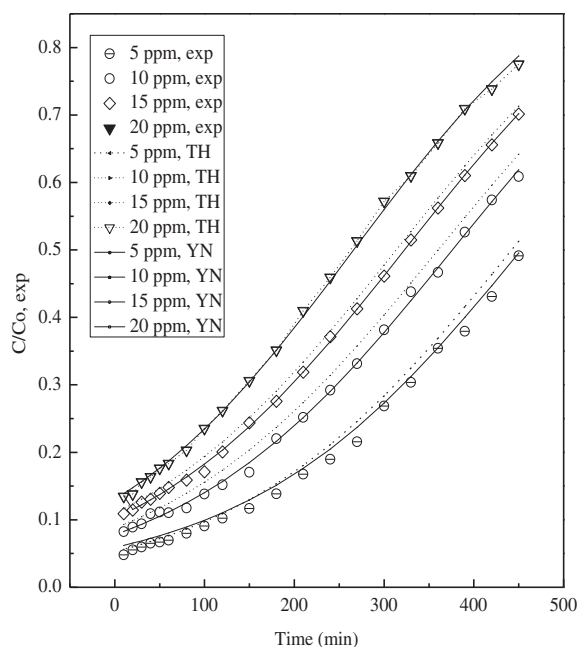


Fig. 16. Effect of initial Cr(VI) concentration on breakthrough performance and comparison with Thomas model and Yoon–Nelson model: flow rate: 15 ml/min, pH 1.5, bed height: 7 cm.

assumes Langmuir kinetics of adsorption–desorption and no axial dispersion, is derived with an assumption that it follows second-order reversible reaction kinetics. In general, the adsorption is not limited by chemical reaction kinetics, but also is often controlled by interphase mass transfer; it leads error when used to model the adsorption process [49].

The non-linear form of the equation is expressed by the equation:

$$\frac{C_t}{C_0} = \frac{1}{1 + \exp\left[K_{th}\left(\frac{q_0\lambda - C_0V_{eff}}{v}\right)\right]} \quad (20)$$

or,

$$\ln\left(\frac{C_0}{C_t} - 1\right) = \frac{K_{th}q_0\lambda}{v} - \frac{K_{th}C_0V_{eff}}{v} \quad (21)$$

The kinetic coefficient,  $K_{th}$  and the adsorption capacity,  $q_0$  are determined from plot of  $\ln(C_0/C_t - 1)$  against  $V_{eff}$  at a given flow rate. The model parameters and correlation co-efficients are shown in Table 8. This model agrees well with the experimental data in the range of  $C_t/C_0 < 0.3$ . This model assumes that the external and internal diffusion is not the limiting step and the Langmuir isotherm is valid. From Table 8, it is clear that as flow rate is increased, equilibrium adsorption capacity increases in line with the experimental values. The correlation coefficients are in the range of 0.92–0.99, and shows good correlation of the experimental data and Thomas model. At increased bed depth, the values of  $K_{th}$  became smaller while the values of  $q_0$  increased. The values of  $K_{th}$  increase with increase in flow rate, but decrease with bed height and initial metal ion concentration. Adsorption capacity,  $q_0$  depends upon the quantity of adsorbent present in the column and increases with increase in flow rate and concentration and decreases with bed height.

3.3.2.2. *Yoon–Nelson model* [50]. This model assumed that the rate of decrease in the probability of adsorption for each adsorbate molecule is proportional to the probability of adsorbate and also probability of adsorbate breakthrough on the adsorbent. The model is expressed as:

Table 8  
Thomas and Yoon–Nelson model parameter at different flow conditions

$Q$ (ml/min)	$C_0$ (mg/l)	$Z$ (cm)	$q_{e,exp}$	% Removal	$q_0$ (mg/g)	$K_{th}$ (l/mg min)	$R^2$ for Thomas model	$k_{YN}$ (min <sup>-1</sup> )	$\tau$ (min)	$R^2$ for Yoon–Nelson model
5	10	5	7.0	99	16.3	0.00101	0.98	0.0152	701.9	0.97
10	10	5	13.28	90.4	15.33	0.00230	0.97	0.0178	502.3	0.96
20	10	5	8.07	26.89	8.54	0.00473	0.99	0.0401	125.4	0.98
15	10	3	18.89	54.34	19.23	0.00105	0.99	0.0081	264.2	0.97
15	10	5	15.55	74.5	18.29	0.00102	0.99	0.0079	407.5	0.97
15	10	7	11.22	75.28	13.33	0.00099	0.98	0.0075	420.9	0.98
15	10	9	9.42	81.34	12.06	0.00094	0.98	0.0079	615.9	0.98
15	5	7	6.89	76.87	8.82	0.00140	0.96	0.0064	459.4	0.98
15	15	7	15.84	67.6	17.91	0.00050	0.94	0.0067	322.7	0.99
15	20	7	17.76	54.09	18.75	0.00041	0.92	0.0071	266.1	0.99

$$\frac{C_t}{(C_0 - C_t)} = \exp(k_{YN}t - k_{YN}\tau) \quad (22)$$

Using linear plot of  $\ln(C_0/C_t - 1)$  vs. time  $t$ , at different flow rate, initial Cr(VI) ion concentration and bed height the values of  $k_{YN}$  and  $\tau$  are determined. The parameters are presented in Table 8 along with Thomas parameters. The correlation coefficient values vary in the ranges of 0.97–0.99, which indicates applicability of the model. The rate constant  $k_{YN}$  values increased with increased in flow rate and concentration, but decreased with increase in bed height. The 50% breakthrough time,  $\tau$ , min decreased considerably with increase in flow rate and initial metal ion concentration. It increased with increase in bed height. Similar results are also obtained by other researchers [18,41].

Figs. 14–16 show the experimental breakthrough plots for various operating condition and also predicted breakthrough curves using Thomas and Yoon–Nelson Model. Based on the correlation coefficient, it may be concluded that Yoon–Nelson model predicts the experimental data slightly better than the Thomson model.

#### 3.4. Safe disposal of the Cr(VI)-loaded adsorbent

The Cr(VI)-loaded rubber leaf disposal in the open atmosphere is not recommended due to possibility of leaching of Chromium ions. Hence, the Cr(VI)-loaded adsorbents are first incinerated at 700°C and then 5 mg of ash samples were mixed with 25 ml of deionized water to give a liquid–solid ratio of 5 [51]. After continuous gentle stirring for 24 h, the filtrate was analyzed for Cr(VI) ions [51]. It was observed that Cr(VI) did not leach from the ash sample. So this ash may be used to fill in the road particularly in the nearby rural areas or place it to the nearby agricultural field. So the ash formation of the used adsorbent will lead to the safe disposal.

#### 4. Conclusions

This study demonstrated the potency of dry rubber leaf in the Cr(VI) removal from aqueous solution. Batch and continuous column experiments were conducted using rubber leaf, a locally available waste, for removal of Cr(VI) from aqueous solution at different process parameters, like pH, adsorbent dose, initial metal ion concentration, contact time etc. in batch operation and different bed height, initial metal ion concentration, and flow rates in continuous column mode. The results may be summarized as follows:

- (1) The removal of Cr(VI) from aqueous solution strongly depends upon pH of the solution. The optimum pH for removal of Cr(VI) on rubber leaf powder was found at pH 1.5.
- (2) The point of zero charge on the adsorbent surface is 7.01.
- (3) Almost 100% removal of Cr(VI) was possible at specified process parameters both in batch and column mode.
- (4) The kinetic process was best described by the pseudo-second-order model with correlation coefficient 0.99.
- (5) Langmuir adsorption isotherm was better fitted than Freundlich model, which indicates that the monolayer adsorption took place.
- (6) Thermodynamic parameters show that the adsorption was spontaneous and endothermic in nature.
- (7) Desorption studies indicate that the rubber leaf powder may be used consecutive three times and after second regeneration, Cr(VI) removal percentage was 79.4%.
- (8) Column studies show that breakthrough curves were affected by flow rate, bed height, and initial metal ion concentration. Increase in flow rate decreased the Cr(VI) removal efficiency due to less contact time, and exhaustion rate of adsorbent was faster at higher flow rates whereas increase in bed height improved removal efficiency.
- (9) Adsorption data slightly better fitted with Yoon–Nelson model compared to Thomas model.
- (10) The study suggests the use of rubber leaf powder as potential adsorbent for removal of Cr(VI) from aqueous solution.

#### Nomenclature

$b$	— langmuir constant (l/mg)
$C_{ad}$	— adsorbed concentration (mg/l)
$C_0$	— influent metal ion concentration at $t = 0$ (mg/l)
$C_t$	— effluent metal ion concentration at time $t$ (mg/l)
$C_t/C_0$	— relative concentration (dimensionless)
$D_e$	— effective diffusion co-efficient of adsorbate in the adsorbent phase ( $m^2/s$ )
$\Delta pH$	— difference of pH
$\Delta G^\circ$	— gibbs free energy (kJ/mol)
$\Delta H^\circ$	— enthalpy (kJ/mol)
$\Delta S^\circ$	— entropy (kJ/(mol/K))
$K_{ad}$	— lageregren rate constant ( $min^{-1}$ )

$K_1, K_2,$ and $K_3$	— equilibrium constant in Eqs. (1)–(3)
$K_2$	— pseudo-second-order rate constant (mg/g/min)
$K_{bq}$	— the constant obtained by multiplying $q_{\max}$ and $b$
$K_c^0$	— thermodynamic equilibrium constant
$K_c'$	— apparent equilibrium constant
$K_{th}$	— thomas rate constant (ml/min mg)
$k_{YN}$	— yoon–Nelson rate constant ( $\text{min}^{-1}$ )
$M$	— mass of the adsorbent per unit volume (g/l)
$m_{\text{total}}$	— total amount of metal sent to the column (mg)
$n$	— freundlich constant, intensity of adsorption $[(\text{mg/g})/(\text{mg/l})]^{1/n}$
$q_0$	— maximum metal uptake per gram of the adsorbent (mg/g)
$q_{eq}$	— equilibrium metal uptake by adsorbent (mg/g)
$q_t$	— total adsorbed Cr(VI) at time $t$ (mg)
$q_{t0}$	— total adsorbed Cr(VI) at time $t = 0$ (mg)
$R$	— percentage removal of metal ion (%)
$Q$	— flow rate (ml/min)
$R^2$	— correlation coefficient
$R$	— ideal gas constant (kJ/mol/K)
$R_L$	— separation factor
$R_a$	— radius of adsorbent particle (m)
$S_s$	— external surface area of the adsorbent per unit volume ( $\text{m}^{-1}$ )
$t$	— time (min)
$t_{\text{total}}$	— total time (min)
$T$	— temperature (K)
$v$	— flow rate (ml/min)
<i>Greek letters</i>	
$\beta$	mass transfer co-efficient (cm/s)
$\tau$	time required for 50% breakthrough (min)
$\chi$	amount of adsorbent present in the column (g)

## References

- [1] US Department of Health and Human Services, Toxicological Profile for Chromium, Public Health Services Agency for the Toxic Substances and Diseases Registry, Washington, DC, 1991.
- [2] M. Cieslak-Golonka, Toxic and mutagenic effects of chromium (VI), *Polyhedron* 15 (1995) 3667–3689.
- [3] C. Raji, T.S. Anirudhan, Batch Cr(VI) removal by polyacrylamide-grafted sawdust: Kinetics and thermodynamics, *Water Res.* 32 (1998) 3772–3780.
- [4] Indian Standard, Drinking Water-specification (first revision), IS 10500, 1991.
- [5] A.K. Bhattacharyya, T.K. Naiya, S.N. Mandal, S.K. Das, Adsorption kinetics and equilibrium studies on removal of chromium(VI) from aqueous solutions using different low-cost adsorbents, *Chem. Eng. J.* 137 (2008) 529–541.
- [6] M. Dakiky, M. Khamis, A. Manassra, Selective adsorption of chromium(VI) in industrial wastewater using low-cost abundantly available adsorbents, *Adv. Environ. Res.* 6 (2002) 533–540.
- [7] M. Emine, Y. Nuhoglu, M. Dundar, Adsorption of chromium (VI) on pomace—An olive oil industry waste: Batch and column studies, *J. Hazard. Mater.* B138 (2006) 142–151.
- [8] B. Singha, S.K. Das, Biosorption of Cr(VI) ions from aqueous solutions: Kinetics, equilibrium, thermodynamics and desorption studies, *Colloids Surf., B* 84 (2011) 221–232.
- [9] S. Chen, Q. Yue, B. Gao, Q. Li, X. Xu, K. Fu, Adsorption of hexavalent chromium from aqueous solution by modified corn stalk: A fixed-bed column study, *Bioresour. Technol.* 113 (2012) 114–120.
- [10] W.K.A.W.M. Khalir, M.A.K.M. Hanafiah, S.Z.M. Sad, W.S.W. Ngah, Z.A.A. Majid, Batch, column and thermodynamics of Pb(II) adsorption on Xanthated Rubber (*Hevea brasiliensis*) leaf powder, *J. Appl. Sci.* 12 (2012) 1142–1147.
- [11] W.S.W. Ngah, M.A.K.M. Hanafiah, Surface modification of rubber (*Hevea brasiliensis*) leaves for the adsorption of copper ions: Kinetic, thermodynamic and binding mechanisms, *J. Chem. Technol. Biotechnol.* 84 (2009) 192–201.
- [12] Standard Methods for Examination of Water and Wastewater, 20th ed., APHA, AWWA, Washington, DC, 1998.
- [13] V.C. Srivastava, I.D. Mall, I.M. Mishra, Characterization of mesoporous rice husk ash (RHA) and adsorption kinetics of metal ions from aqueous solution onto RHA, *J. Hazard. Mater.* B134 (2006) 257–267.
- [14] A.A. Attia, S.A. Khedr, S.A. Elkholy, Adsorption of chromium ion (VI) by acid activated carbon, *Braz. J. Chem. Eng.* 27(1) (2010) 183–193.
- [15] S. Babel, T.A. Kurniawan, Cr(VI) removal from synthetic waste water using coconut shell charcoal and commercial activated carbon modified with oxidizing agents and/or chitosan, *Chemosphere* 54 (2004) 951–967.
- [16] K. Mohanty, M. Jha, B.C. Meikap, M.N. Biswas, Biosorption of Cr(VI) from aqueous solutions by *Eichhornia crassipes*, *Chem. Eng. J.* 117 (2006) 71–77.
- [17] Y.C. Sharma, Adsorption of Cr(VI) onto wollastonite: Effect of pH, *Indian J. Chem. Technol.* 8 (2001) 186–190.
- [18] E. Malkoc, Y. Nuhoglu, Y. Abali, Cr(VI) adsorption by waste acorn of *Quercus ithaburensis* in fixed beds: Prediction of breakthrough curves, *Chem. Eng. J.* 119(1) (2006) 61–68.
- [19] D. Balarak, Y. Mahdavi, F. Gharlbi, S. Sedeghi, Removal of hexavalent chromium from aqueous solution using canola biomass: Isotherms and kinetics studies, *J. Adv. Environ. Health Res.* 2(4) (2014) 1–8.
- [20] P. Miretzky, A.F. Cirelli, Cr(VI) and Cr(III) removal from aqueous solution by raw and modified lignocellulosic materials: A review, *J. Hazard. Mater.* 180 (1–3) (2010) 1–19.
- [21] S. Lagergren, Zur theorie der sogenannten adsorption gelöster stoffe, *Handlingar* 24 (1898) 1–39.
- [22] Y.S. Ho, G. McKay, D.A.J. Wase, C.F. Forster, Study of the sorption of divalent metal ions on to peat, *Adsorpt. Sci. Technol.* 18 (2000) 639–650.
- [23] E. W. Wambu, G.K. Muthakia, J.K. wa-Thiong'o, P.M. Shiundu, Kinetic and thermodynamics of aqueous

- Cu(II) adsorption on heat regenerated spent bleaching earth, *Bull. Chem. Soc. Ethiop.* 25(2) (2011) 181–190.
- [24] G. McKay, M.S. Otterburn, A.G. Sweeney, Surface mass transfer processes during colour removal from effluent using silica, *Water Res.* 15 (1981) 327–331.
- [25] I.A.W. Tan, A.L. Ahmad, B.H. Hameed, Adsorption of basic dye on high-surface-area activated carbon prepared from coconut husk: Equilibrium, kinetic and thermodynamic studies, *J. Hazard. Mater.* 154(1–3) (2008) 337–346.
- [26] M.M. El-Latif, A.M. Ibrahim, M.S. Showman, R.R.A. Hamide, Alumina/iron oxide nano composite for cadmium ions removal from aqueous solutions, *Int. J. Nonferrous Metall.* 2 (2013) 47–62.
- [27] I. Langmuir, The adsorption of gases on plane surfaces of glass, mica and platinum, *J. Am. Chem. Soc.* 40 (1918) 1361–1403.
- [28] M.M. Dubinin, E.D. Zaverina, L.V. Radushkevich, Sorption and structure of active carbons I. Adsorption of organic vapors, *Zh. Fiz. Khim.* 21 (1947) 1351–1362.
- [29] M.F. Sawalha, J.R. Peralta-Videa, J. Romero-González, J.L. Gardea-Torresdey, Biosorption of Cd(II), Cr(III), and Cr(VI) by saltbush (*Atriplex canescens*) biomass: Thermodynamic and isotherm studies, *J. Colloid Interface Sci.* 300 (2006) 100–104.
- [30] H. Nollet, M. Roels, P. Lutgen, P. Van der Meeren, W. Verstraete, Removal of PCBs from wastewater using fly ash, *Chemosphere* 53(6) (2003) 655–665.
- [31] N. Ahalya, R.D. Kanamadi, T.V. Ramachandra, Biosorption of chromium (VI) by *Tamarindus indica* pod shells, *J. Environ. Sci. Res. Int.* 1(2) (2008) 77–81.
- [32] S.H. Hasan, K.K. Singh, O. Prakash, M. Talat, Y.S. Ho, Removal of Cr(VI) from aqueous solutions using agricultural waste 'maize bran', *J. Hazard. Mater.* 152 (2008) 356–365.
- [33] D.C. Sharma, C.F. Forster, A preliminary examination into the adsorption of hexavalent chromium using low-cost adsorbents, *Bioresour. Technol.* 47(3) (1994) 257–264.
- [34] G. Cimino, A. Passerini, G. Toscano, Removal of toxic cations and Cr(VI) from aqueous solution by hazelnut shell, *Water Res.* 34 (2000) 2955–2962.
- [35] M. Dakiky, M. Khamis, A. Manassra, M. Mer'eb, Selective adsorption of chromium (VI) in industrial wastewater using low-cost abundantly available adsorbents, *Adv. Environ. Res.* 6 (2002) 533–540.
- [36] T. Karthikeyan, S. Rajgopal, L.R. Miranda, Chromium (VI) adsorption from aqueous solution by *Hevea brasiliensis* sawdust activated carbon, *J. Hazard. Mater.* 124(1–3) (2005) 192–199.
- [37] M. Nameni, M.R. Alavi Moghadam, M. Arami, Adsorption of hexavalent chromium from aqueous solutions by wheat bran, *Int. J. Environ. Sci. Technol.* 5(2) (2008) 161–168.
- [38] C.P. Huang, M.H. Wu, The removal of chromium(VI) from dilute aqueous solution by activated carbon, *Water Res.* 11 (1977) 673–679.
- [39] Y. Orhan, H. Büyükgüngör, The removal of heavy metals by agricultural wastes, *Water Sci. Technol.* 28 (2) (1993) 247–255.
- [40] K. Morshedzadeh, H.R. Soheilzadeh, S. Zangoie, M. Aliabadi, Removal of chromium from aqueous solutions by lignocellulosic solid wastes, in: First Environment Conference, Department of Environmental Engineering, Tehran University, Iran, 2007.
- [41] T. Mitra, B. Singha, N. Bar, S.K. Das, Removal of Pb (II) ions from aqueous solution using water hyacinth root by fixed-bed column and ANN modeling, *J. Hazard. Mater.* 273 (2014) 94–103.
- [42] J.T. Nwabanne, P.K. Igbokwe, Adsorption performance of packed bed column for the removal of lead (II) using oil palm fibre, *Int. J. Appl. Sci. Technol.* 2(5) (2012) 106–115.
- [43] I.A.W. Tan, A.L. Ahmad, B.H. Hameed, Adsorption of basic dye using activated carbon prepared from oil palm shell, batch and fixed bed studies, *Desalination* 225(1–3) (2008) 13–28.
- [44] U. Farooq, M. Athar, M.A. Khan, J.A. Kozinski, Biosorption of Pb(II) and Cr(III) from aqueous solutions: Breakthrough curves and modeling studies, *Environ. Monit. Assess.* 185 (2013) 845–854.
- [45] Z. Saddi, R. Saadi, R. Fazaeli, Fixed-bed adsorption dynamics of Pb(II) adsorption from aqueous solutions using nanostructured  $\gamma$ -alumina, *J. Nanostruct. Chem.* 3 (July 2013) 1–8 (Article ID 48).
- [46] F. Kafshgari, A.R. Keshtkar, M.A. Musavian, Study of Mo(VI) removal from aqueous solution: Application of different mathematical models to continuous biosorption data, *Iran. J. Environ. Health Sci. Eng.* 10 (2013) 1–11, Article ID 14.
- [47] B. Singha, S.K. Das, Adsorptive removal of Cu(II) from aqueous solution and industrial effluent using natural/agricultural wastes, *Colloids Surf., B* 107 (2013) 97–106.
- [48] H.G. Thomas, Chromatography: A problem in kinetics, *Ann. N.Y. Acad. Sci.* 49 (1948) 161–182.
- [49] M. Khraisheh, M.A. Al-Ghouti, C.A. Stanford, The application of iron coated activated alumina, ferric oxihydroxide and granular activated carbon in removing humic substances from water and wastewater: Column studies, *Chem. Eng. J.* 161 (2010) 114–121.
- [50] Y.H. Yoon, J.H. Nelson, Application of gas adsorption kinetics I. A theoretical model for respirator cartridge service life, *Am. Ind. Hyg. Assoc. J.* 45 (1984) 509–516.
- [51] D.B. Sarode, R.N. Jadhav, V.A. Khatik, S.T. Ingle, S.B. Attarde, Extraction and leaching of heavy metals from thermal power plant fly ash and its admixtures, *Pol. J. Environ. Stud.* 19(6) (2010) 1325–1330.